Sindh Univ. Res. Jour. (Sci. Ser.) Vol.44 (4) 635- 640 (2012)

SINDH UNIVERSITY RESEARCH JOURNAL (SCIENCE SERIES)

Multiple Model Based Real Time Estimation of Wheel-Rail Contact Conditions

I. HUSSAIN, F. R. ABRO, A.A. MEMON* I.A. MEMON**

Department of Electronic Engineering, Mehran University Jamshoro

Received 24th February 2012 and Revised 22nd September 2012

Abstract: This paper presents the development of a novel and vehicle based technique for the real time estimation of the contact conditions by using multiple models to represent variations in the adhesion level and different contact conditions. The proposed scheme interprets the variations in the dynamic response of the wheelset with the changing adhesion conditions into contact condition information. The proposed system involves the use of a number of carefully selected mathematical models of a rail vehicle to mimic train dynamic behaviours in response to different track conditions. The level of matches/mismatches is reflected in the estimation errors of the models concerned, when compared with the real vehicle. The output residuals from all the models are then assessed to determine the track conditions.

Keywords: Wheel Rail Contact, Estimation, Kalman Filters, Adhesion.

1. INTRODUCTION

The level of adhesion between the wheel and the rail has a major impact on the ability to brake and to accelerate vehicle properly. If the wheels deliver a higher force to the rail than they can transmit, the wheels start to slip in traction or slide in braking causing surface damage to wheels and rails causing additional costs to railway industry.

Several measures have been taken by the railway industry around the world to improve the level of adhesion in severe weather conditions. For example wheel slip/slide protection (WSP) technologies for traction and braking systems are incorporated in the rail vehicles to maximize the use of available adhesion (Watanabe and Yamanaka, 1997). WSPs control the slip ratio (relative speed between a wheel and the train) below a pre-defined threshold to avoid slip/slide during traction and braking. Those controllers are difficult to obtain optimal performance and also require accurate measurement of wheel slip. In general, WSPs are effectively reactive systems, i.e. only 'activated' to stop wheel slip/slide when detected by the sensors. The railway industry in the UK is currently taking formative steps in the use of real time condition monitoring of railway vehicles (Ward, 2011). A number of ideas have been proposed to detect the running condition of the wheel-rail interface (Ward, Xia *et at.,* 2007, Charles *et at.,* 2008). A model based scheme for condition monitoring at the wheel rail interface is proposed in (Charles *et at.,* 2008). The adhesion level is identified by measuring the dynamic response of the vehicle to lateral track irregularities under normal running. This work is further carried out in (Ward) with the primary aim to estimate the creep forces generated at the wheel-rail contact. An inverse modelling approach for the estimation of the creep coefficients using measured car body acceleration is proposed in (Xia *et at.,* 2007).

This paper presents a novel idea to develop a technique for the real time estimation of the wheel-rail contact conditions as the train travels through the track. The idea is based on the fact that the dynamics response of the wheelset is changed with the changes in the wheel-rail contact conditions. The proposed solution exploits the fact that the dynamic behaviour of a railway vehicle is strongly affected by the nonlinearity as well as the variations in the creep characteristics. The purpose of the proposed scheme is to interpret these variations in the dynamic response of the wheelset into useful contact condition information. The proposed system involves the use of a number of carefully selected mathematical models of a rail vehicle to mimic train dynamic behaviours in response to different track conditions. The level of matches/mismatches is reflected in the estimation errors of the models concerned, when compared with the real vehicle. The output residuals from all the models are then assessed to determine the track conditions.

2. Modelling Of System Dynamics

Wheelset is a vital element of railway transport and in direct contact with the track therefore the dynamics of the wheelset are directly influenced by changing contact conditions therefore a single solid axle powered wheelset is considered in this study. In various other stability and guidance studies the primary focus of study is on a single wheelset which can be easily extended to two axles and full vehicle with some modifications (Park *et at.,* 2001, Mei *et at.,* Mei *et at.,* 2009, Charles *et at.,* 2008, Li and Goodall, 1998, Mei and Goodall, 2003, Yu *et at.,* Yu, Iwnicki, 2003, Goodall and Li, 2000, Goodall, 1999, Beagley *et at.,*

++Corresponding author: Corresponding Author: Imtiaz Hussain (imtiaz.hussain@faculty.muet.edu.pk)

*Department of Electrical Engineering Mehran University Jamshoro

**Institute of Physics, University of Sindh, Jamshoro

1975). The simplified plan view of the wheelsets in a bogie frame is shown in **(Fig.1)**. The wheelset is connected to vehicle body or bogie via suspension elements in lateral and longitudinal directions. The longitudinal connections between the wheelset and the bogie are assumed to be solid as the stiffness is normally very high and associated dynamics are not of the significant relevance to this study (Mei *et at.,* 2006). However longitudinal springs provide necessary yaw stiffness to stabilise the kinematic motion of the wheelset. All the forces that govern the dynamic behaviour of the wheelset are generated at the wheel-rail contact patch which is typically very small (about 1 cm^2) (Iwnicki, 2006). These forces are nonlinear function of the creep **(Fig.2),** a phenomenon occurs due to micro-slip in the area of contact, and therefore called creep forces. The creep is defined as the relative speed of the wheels to rail and characterized as the lateral and longitudinal creep in accordance with the direction of motion (Hussain and X, Hussain, 2010).

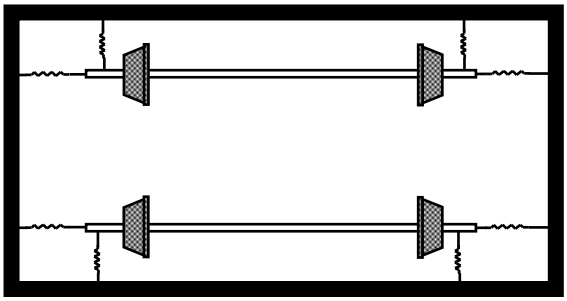

Fig.1: Railway Wheelsets in a Bogie Frame

$$\lambda_{xL} = \frac{r_o\omega_L - v}{v} + [\frac{L_g\dot{\psi}}{v} + \frac{\gamma(y - y_t)}{r_o}] \quad (1)$$

$$\lambda_{xR} = \frac{r_o\omega_R - v}{v} - [\frac{L_g\dot{\psi}}{v} + \frac{\gamma(y - y_t)}{r_o}] \quad (2)$$

$$\lambda_y = \frac{\dot{y}}{v} - \psi \quad (3)$$

where the subscripts L and R represent left and right wheels, r_o is radius of the wheels, v is vehicle forward speed, γ is the conicity of the wheels, ψ is yaw angle, L_g is track half gauge, ω_L and ω_R are the angular velocities of the left and right wheels respectively, y is lateral motion, $\acute{y}$ is speed associated with lateral motion and y_t is track disturbance in lateral direction. The total creepage λ_j is the combination of the lateral and longitudinal creepages.

$$\lambda_j = \sqrt{\lambda_{ij}^2 + \lambda_{ij}^2} \quad i = x, y \text{ and } j = L, R \quad (4)$$

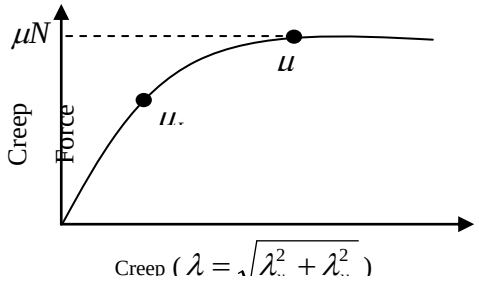

Fig .2: Creep vs Creep Force

(Fig.3) demonstrates how the creep forces are dramatically affected by the presence of a third body layer, e.g. crushed leaves, water, ice and etc, at the wheel-rail contact. This could be formed by a substance to increase/decrease friction or by naturally occurring substance acting to decrease friction. In order to have proper traction and braking performance a minimum level of adhesion (0.25 for traction and up to 0.1 for braking) is required. In poor contact conditions, the maximum adhesion available can be far below what is needed for the normal provision of traction or braking.

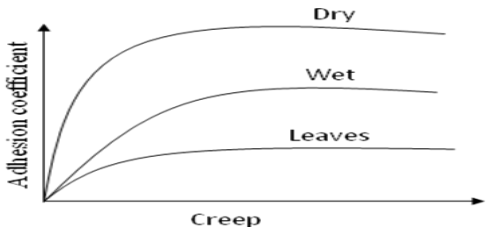

Fig.3: Creep Force affected by contaminations on rail surface

It is essential in the study of wheelset dynamics to develop and use a comprehensive model that include all relevant motions of the wheelset related to the contact forces because of the strong interactions between different motions of the wheelset through the creep forces at the wheel-rail contact acting in both longitudinal and lateral directions. The railway wheelset has several degrees of freedom. The lateral displacement, yaw angle, longitudinal motion and the rotational motion are considered for this study, whereas the roll and bounce motion are constrained by the track and not included in the wheelset model. The dynamic equations are given as follows (Hussain and X, Hussain, 2009, Hussain, 2010).

$$M_v\ddot{x} = \frac{\mu_R N_R}{\sqrt{\lambda_{xR}^2 + \lambda_{yL}^2}}\left[\frac{r_o\omega_{wR} - v}{v} - [\frac{L_g\dot{\psi}}{v} + \frac{\omega_{wR}\gamma(y - y_t)}{v}]\right] + \frac{\mu_L N_L}{\sqrt{\lambda_{xL}^2 + \lambda_{yL}^2}}\left[\frac{r_o\omega_{wL} - v}{v} + [\frac{L_g\dot{\psi}}{v} + \frac{\omega_{wL}\gamma(y - y_t)}{v}]\right] \quad (5)$$

$$I_w\ddot{\psi} = \frac{\mu_R N_R}{\sqrt{\lambda_{xR}^2+\lambda_{yL}^2}}\left[\frac{r_o\omega_{wR}-v}{v}-\left[\frac{L_g\dot{\psi}}{v}+\frac{\omega_{wR}\gamma(y-y_t)}{v}\right]\right]L_g$$
$$-\frac{\mu_L N_L}{\sqrt{\lambda_{xL}^2+\lambda_{yL}^2}}\left[\frac{r_o\omega_{wL}-v}{v}+\left[\frac{L_g\dot{\psi}}{v}+\frac{\omega_{wL}\gamma(y-y_t)}{v}\right]\right]L_g \quad (6)$$
$$-k_w\psi$$

$$m_w\ddot{y} = -\frac{\mu_L N_L}{\sqrt{\lambda_{xL}^2+\lambda_{yL}^2}}\left[\frac{\dot{y}}{v}-\psi\right]-\frac{\mu_R N_R}{\sqrt{\lambda_{xR}^2+\lambda_{yL}^2}}\left[\frac{\dot{y}}{v}-\psi\right] \quad (7)$$

$$I_R\dot{\omega}_R = T_t - K_s\theta_s - r_o\frac{\mu_R N_R}{\sqrt{\lambda_{xR}^2+\lambda_{yL}^2}}\left[\frac{r_o\omega_{wR}-v}{v}-\left[\frac{L_g\dot{\psi}}{v}+\frac{\omega_{wR}\gamma(y-y_t)}{v}\right]\right] \quad (8$$

where $\theta_s = \int(\omega_R-\omega_L)dt$

$$I_L\dot{\omega}_L = K_s\theta_s - r_o\frac{\mu_L N_L}{\sqrt{\lambda_{xL}^2+\lambda_{yL}^2}}\left[\frac{r_o\omega_{wL}-v}{v}+\left[\frac{L_g\dot{\psi}}{v}+\frac{\omega_{wL}\gamma(y-y_t)}{v}\right]\right] \quad (9)$$

3. MATERIAL AND METHODS

Model Based Estimation

Model based estimation uses the knowledge of a system in the form of a mathematical model and measured response(s) to input to perform real-time estimation of the system parameters of interest (Charles *et at.*, 2008). This section presents the use of model based detection for estimating the wheel rail contact conditions. The proposed system, shown in **(Fig.4),**

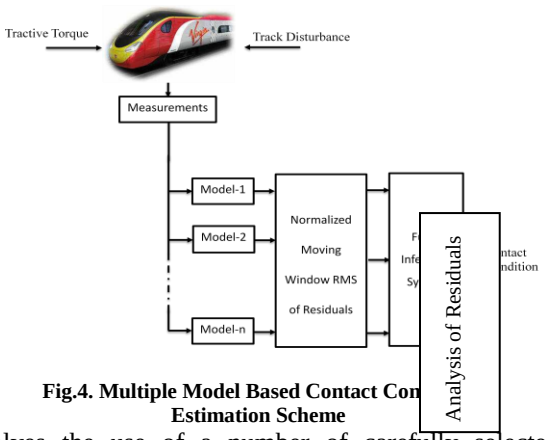

Fig.4. Multiple Model Based Contact Con
Estimation Scheme

involves the use of a number of carefully selected mathematical models of a rail vehicle to mimic train dynamic behaviours in response to different track conditions. Each of the estimators is tuned to match one particular track condition to give the best results at the specific design point. Increased estimation errors are expected if the contact condition is not at or near the chosen operating point. The level of matches/mismatches is reflected in the residuals of the models concerned, when compared with the real vehicle through the measurement output of vehicle mounted inertial sensors. The output residuals from all the models are then assessed to determine which of the models provide a best match to the present operating condition and hence to give real time information about the track conditions.

3.1 Simplification Of Wheelset Dynamics

For practicality purpose it is necessary that the design of the estimators should be as simple as possible by considering the wheelset dynamics which are directly related to contact condition. Previous studies have shown that the lateral and yaw dynamics are sufficient to detect these changes (Charles and Goodall, 2007, Mei and Goodall, 2002, Charles *et at.*, 2008, Yu, Mei and Hussain, 2010, I Hussain, Hussain, 2010). Therefore for the estimator design some simplifications in the wheelset model are introduced. The simplified dynamic equations involving only yaw and lateral dynamics are given below.

$$I_w\ddot{\psi} = \frac{\mu_R N_R}{\sqrt{\lambda_{xR}^2+\lambda_{yL}^2}}\left[-\frac{L_g\dot{\psi}}{v}+\frac{\gamma(y-y_t)}{r_o}\right]L_g \quad (10)$$
$$-\frac{\mu_L N_L}{\sqrt{\lambda_{xL}^2+\lambda_{yL}^2}}\left[\frac{L_g\dot{\psi}}{v}+\frac{\gamma(y-y_t)}{r_o}\right]L_g - k_w\psi$$

$$m_w\ddot{y} = -\frac{\mu_L N_L}{\sqrt{\lambda_{xL}^2+\lambda_{yL}^2}}\left[\frac{\dot{y}}{v}-\psi\right]-\frac{\mu_R N_R}{\sqrt{\lambda_{xR}^2+\lambda_{yL}^2}}\left[\frac{\dot{y}}{v}-\psi\right] \quad (11)$$

The simplified model has several advantages in estimator design without having a significant effect on the results (Mei and Hussain, 2010, I Hussain, 2010). The major advantage is the simple design of the estimator with minimum number of states which will allow the estimator to converge quickly. The yaw and lateral dynamics are excited by lateral track irregularities hence no torque input is required to estimators in simplified model.

Since the adhesion coefficient μ has nonlinear relationship with the creep, therefore the equation (10) and (11) are linearized at (λ_{xo}, λ_{yo}) under the assumption that the left and right wheels have same contact condition and small signal model of lateral and yaw dynamics of the wheelset is obtained.

$$\Delta\ddot{\psi} = -\frac{2L_g^2 g_{11}}{vI_w}\Delta\dot{\psi}-\frac{2L_g g_{11}\gamma}{r_o I_w}\Delta y+\frac{2L_g g_{11}\gamma}{r_o I_w}\Delta y_t \quad (12)$$
$$-\frac{k_w}{I_w}\Delta\psi$$

$$\Delta\ddot{y} = -\frac{2g_{22}}{m_w v}\Delta\dot{y}+\frac{2g_{22}}{m_w}\Delta\psi \quad (13)$$

The final small signal model of the simplified wheelset model is given in following equation in the state space form.

$$\frac{d}{dt}\begin{bmatrix}\Delta y\\ \Delta\psi\\ \Delta\dot{y}\\ \Delta\dot{\psi}\end{bmatrix}=\begin{bmatrix}0 & 0 & 1 & 0\\ 0 & 0 & 0 & 1\\ 0 & \frac{2g_{22}}{m_w} & -\frac{2g_{22}}{vm_w} & 0\\ -\frac{2L_g\gamma g_{11}}{r_o I_w} & -\frac{k_w}{I_w} & 0 & -\frac{2L_g^2 g_{11}}{vI_w}\end{bmatrix}\begin{bmatrix}\Delta y\\ \Delta\psi\\ \Delta\dot{y}\\ \Delta\dot{\psi}\end{bmatrix}+\begin{bmatrix}0\\ 0\\ 0\\ \frac{2L_g\gamma g_{11}}{r_o I_w}\end{bmatrix}\Delta y_t \quad (14)$$

Where g_{11} and g_{22} represent the slope of the creep curve at operating point. From the equation (14) it is clear that the dynamics of the wheelset are dependent upon the changes in the contact condition. More significantly the dynamics of the wheelset varies with the changes in the operating point of the wheelset and depend upon the slope of the creep curve and the traction ratio at the point where wheelset is operating. This shows that not only a change in contact condition has significant effect on wheelset dynamics but the dynamics are also varied during the application of traction and braking. Therefore it is important to monitor the tractive effort and the wheelset dynamics together in order to identify the available contact conditions.

3.2 Estimator Design

The most commonly used state estimator is the Kalman filter. Kalman Bucy filter (which is a continuous time counterpart of the discrete Kaman filter) is chosen for this research because it gives good results due to optimality and robustness in presence of stochastic noises applied by the track, it is convenient for online real time processing and it is easy to formulate and implement given a basic understanding. A Kalman filter based on small signal model of equation (14) can be designed to estimate the states of the system at specific point on the creep curve. Nevertheless this is not a trivial application of the Kalman filter because the track irregularities y_t that excite the lateral and yaw dynamics of the railway wheelset are not directly measurable (Charles *et at.*, 2008) and cannot be neglected either, which makes the design of the Kalman filter more complex. Therefore the equation (14) is reformulated where the unknown parameter y_t is treated as part of the state vector such that the dynamics of the system are remained unchanged (Mei and Goodall, 2002, Mei T. X.).

Equation (15) shows the reformulated model where y_t is treated as part of the state vector by assuming

$$\frac{d}{dt}\begin{bmatrix}\Delta\psi\\ \Delta\dot{y}\\ \Delta\dot{\psi}\\ \Delta y_t\\ \Delta y-\Delta y_t\end{bmatrix}=\begin{bmatrix}0 & 0 & 1 & 0 & 0\\ \frac{2g_{22}}{m_w} & -\frac{2g_{22}}{vm_w} & 0 & 0 & 0\\ -\frac{k_w}{I_w} & 0 & -\frac{2L_g^2 g_{11}}{vI_w} & 0 & -\frac{2L_g\gamma g_{11}}{r_o I_w}\\ 0 & 0 & 0 & N & 0\\ 0 & 1 & 0 & 0 & 0\end{bmatrix}\begin{bmatrix}\Delta\psi\\ \Delta\dot{y}\\ \Delta\dot{\psi}\\ \Delta y_t\\ \Delta y-\Delta y_t\end{bmatrix}+\begin{bmatrix}0\\ 0\\ 0\\ 1\\ -1\end{bmatrix}\Delta\dot{y}_t \quad (15)$$

$\Delta\dot{y}_t = N\Delta y_t + \Delta\dot{y}_t$, where N is a small constant added to the system to keep the system matrix full ranked. Two sensors (A gyro sensor for yaw rate measurement and an accelerometer for lateral acceleration measurement) as indicated in equation (16) have been found to be sufficient for Kalman filter to provide satisfying estimation results (Hussain, 2009, Hussain, 2010, Hussain and X).

$$z(t)=\begin{bmatrix}0 & 0 & 1 & 0 & 0\\ \frac{2g_{22}}{m_w} & -\frac{2g_{22}}{vm_w} & 0 & 0 & 0\end{bmatrix}\begin{bmatrix}\Delta\psi\\ \Delta\dot{y}\\ \Delta\dot{\psi}\\ \Delta y_t\\ \Delta y-\Delta y_t\end{bmatrix}+v \quad (16)$$

where v is a vector representing noise level of sensors. It is assumed that there is no correlation between process and measurement noises. As we know the detection algorithm is formulated based on the multiple model approach. Therefore the Kalman filters are designed to operate in different contact conditions, as shown in figure-5, by tuning the Kalman filter parameters (R measurement noise covariance, Q process noise covariance and N small constant) and the contact condition parameters (g_{11} and g_{22}). Four Kalman filters are found to be sufficient to detect the changes in the contact conditions. The creep curves shown in following figure are used for the basis of the study. The Kalman filters are tuned to operate on saturation region of each creep curve.

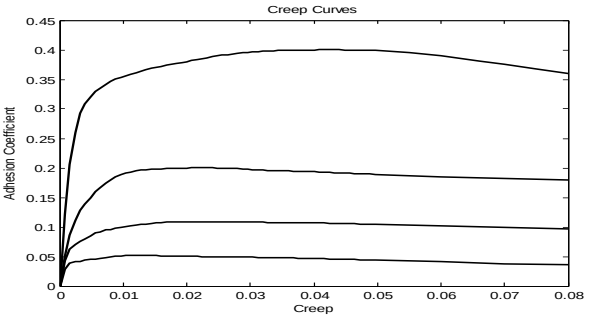

Fig.5.Creep curves used to design the Kalman filters

4. RESULTS AND DISCUSSION

Simulation Results Simulations are run using creep curves shown in **(Fig.5)** and the normalized rms values of the residuals with moving time window of one second are calculated.

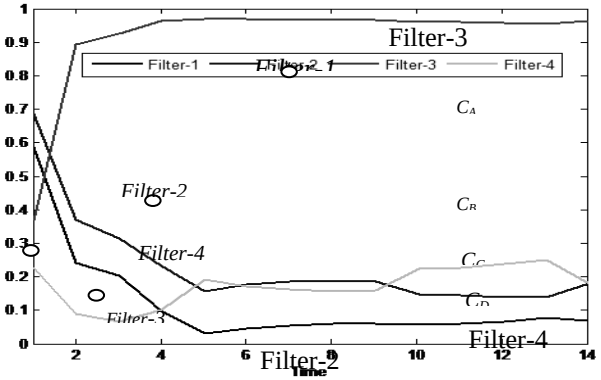

Fig.6. Residuals of filters at saturation region of C_A

(Fig.6) shows the residuals of the filters when the wheelset is operated at the saturation region of the creep curve C_A. The residual of filter-1 is minimum because filter-1 is designed to operate at this operating point. The residuals of filter-2 and filter-4 are relatively large and the residual of filter-3 is very high because this filter is designed to operate at very low adhesion conditions. When the wheelset is operated at the saturation point of the creep curve C_C the residual of filter-2 is decreased and has minimum value as compare to rest of the filters. The residual of the filter-1 is increased whereas residual of filter-3 tend to decrease as the adhesion level is decreased. The result of the simulation is shown in **(Fig.7).**

When the adhesion level is further reduced to 5% the residuals of the filter-1, filter-2 are increased and reached to their maximum value whereas the residual of filter-3 has minimum value **(Fig. 8and 9)** indicating that the vehicle is now operating in low adhesion conditions. If the wheelset is not operated on the saturation points of the creep curves the residual of filter-4 should be minimum because the design of filter-4 is based on high coefficient values (g_{11}, g_{22}). For instance when the wheelset is operated in the linear region of the creep curve C_A the residual of filter-4 is minimum as shown in figure-9. In this way filter-4 provides the information to the decision making system to make sure if the wheelset operating point is reached to saturation point in order to make a correct decision.

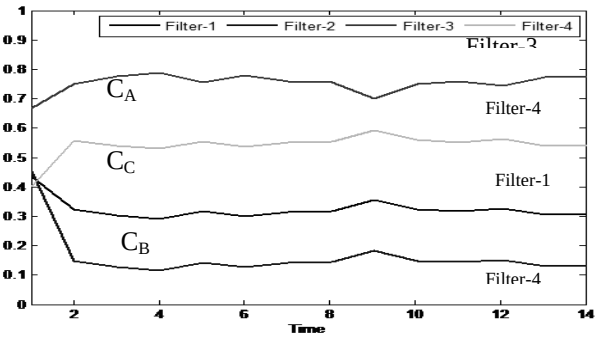

Fig.7. Residuals of filters at saturation region of C_C

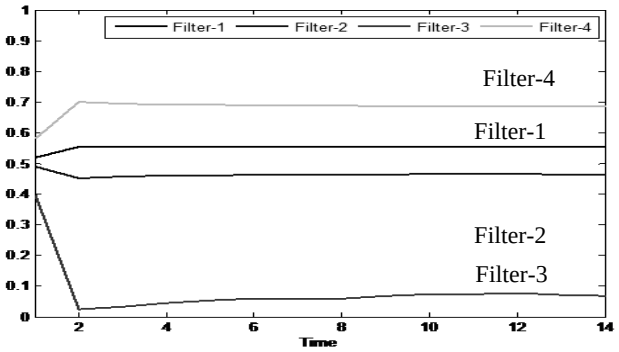

Fig.8.Residuals of filters at saturation region of C_D

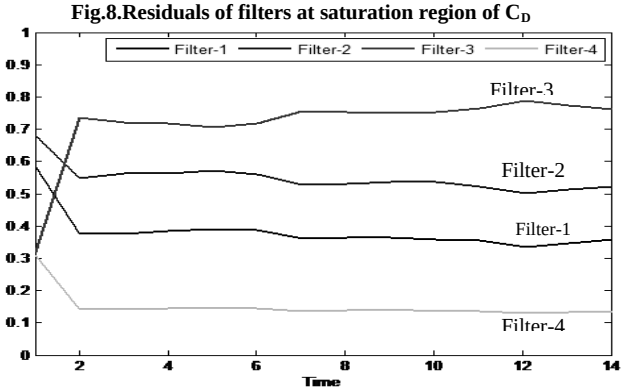

Fig.9. Residuals of filters when the wheelset is operated in the linear region of C_A

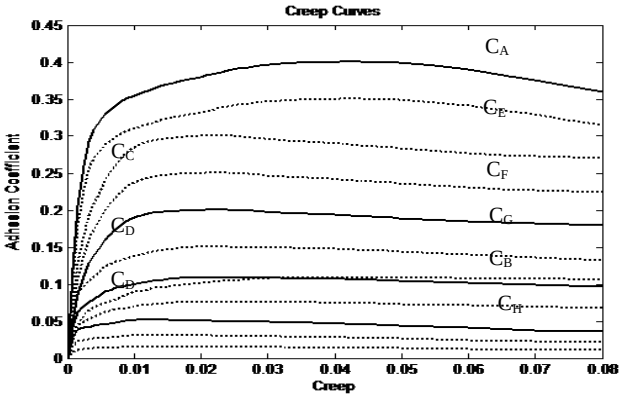

Fig.10. Creep Curves

Table-1 Residual Values

No.	Adhesion (μ%)	Filter-1	Filter-2	Filter-3	Filter-4
1	C_A (40%)	0.08	0.2	0.95	0.2-0.3
2	C_E (35%)	0.09	0.2	0.95	0.25-0.35
3	C_F (25%)	0.12	0.25	0.9	0.15-0.25
4	C_B (20%)	0.08	0.2	0.9	0.2-0.4
5	C_G (15%)	0.22	0.15	0.8	0.25-0.55
6	C_C (10%)	0.25	0.1	0.8	0.2-0.6
7	C_D (5%)	0.32	0.12	0. 8	0.6-0.65
8	C_H (3%)	0.5	0.4	0.12	0.72

In general when the vehicle operates in a contact condition similar to filter-1 the residual of filter-1 is smaller as compare to rest of the models and in this way the information about the contact condition

is reflected in the residual values. But we have used only four models and there are infinite possibilities for contact conditions. Therefore the scheme is simulated using variety of different contact conditions shown in **(Fig.10)** and the residual values are given in table-1. **(Table-1)** shows that the residuals tend to have different values at different levels of adhesion and based on these results a decision making system can be developed that can interpret these variations in the residuals into adhesion level information.

5. CONCLUSIONS AND FURTHER WORK

The good delivery of the attractive effort in the traction and braking can be achieved through the real time knowledge of the contact condition. This research proposes a novel technique to identify the contact condition by investigating the changes in the dynamic properties of the wheelset as the train travel through the track. The proposed scheme indirectly identifies the contact condition minimum measurement requirement. The results presented the satisfactory performance. Further research is been carried out to experimentally validate this model in different contact conditions.

REFERENCES:

Bombardier, M. (2010) Orbita–Predictive et Management, The Future Of Fleet Maintenance, Http://www. Bombardier.Com/En/Transportation/,Accessed 7th April

Beagley, T., I. Mcewen, and C. Pritchard, (1975) Wheel/Rail Adhesion--Boundary Lubrication By Oily Fluids. *Wear,* 31**,** 77-88.

Charles, G. and R. oodall, (2007) Year. Low Adhesion Estimation. *In*,. Iet, 96-101.

Charles, G., R. Goodall, and R.Dixon, (2008) Model-Based Condition Monitoring At The Wheel-Rail Interface. *Vehicle System Dynamics,* 46**,** 415-430.

Christopher R. G. and A. R. D. Ward, (2011) Creep Force Estimation At The Wheel-Rail Interface. *Proceedings Of The 22nd International Symposium On Dynamics Of Vehicles On Roads And Tracks*. 14-19

Goodall, R. (1999) Tilting Trains And Beyond. The Future For Active Railwaysuspensions. 2. Improving Stability And Guidance. *Computing and Control Engineering Journal,* **(10)**: 221-230.

Goodall, R. and H. Li, (2000) Solid Axle And Independently-Rotating Railway Wheelsets-A Control Engineering Assessment Of Stability. *Vehicle System Dynamics,* **(33):** 57-67.

Hussain, I. (2011) Identification Of The Wheel Rail Contact Condition For The Traction And Braking Control *Proceedings Of The 22nd International Symposium On Dynamics Of Vehicles On Roads And Tracks, Manchester Metropolitan University,* 14-19.

Hussain, M. T. X. (2010) Multi Kalman Filtering Approach For Estimation Of Wheel-Rail Contact Conditions *Proceedings Of The United Kingdom Automatic Control Conferecne,* 459-464.

Hussain, M. T. X. (2009) Modeling And Estimation Of Nonlinear Wheel-Rail Contact Mechanics. *Proceedings Of The Twentieth Intenational Conference On System Engineering***,** 219-223.

Iwnicki, S. (2003) Simulation Of Wheel-Rail Contact Forces. *Fatigue & Fracture Of Engineering Materials & Structures,* **(26)**: 887-900.

Li, H. and R. Goodall, (1998) Year. Modelling And Analysis Of A Railway Wheelset For Active Control. *In*, 1289-1293.

Mei, T. and R. Goodall, (2002) Ga Solutions For Active Steering Of Railway Vehicles. *In*, Iet, 111-117.

Mei, T., J. Yu, and D. Wilson, (2006) Wheelset Dynamics And Wheel Slip Detection. *Chengdu, China*.

Mei, T., J. Yu, and D.Wilson, (2009) A Mechatronic Approach For Effective Wheel Slip Control In Railway Traction. *Proceedings Of The Institution Of Mechanical Engineers, Part F: Journal Of Rail And Rapid Transit,* **(223):** 295-304.

Mei, T. X. and R. M. Goodall, (2003) Practical Strategies For Controlling Railway Wheelsets Independently Rotating Wheels. *Journal Of Dynamic Systems, Measurement, And Control,* **(125)**: 354-360.

Mei, T. X. and I. Hussain, (2010) Year. Detection Of Wheel-Rail Conditions For Improved Traction Control. *In:* Railway Traction Systems (Rts 2010), Iet Conference On, 13-15. 1-6.

Park, K. T., H. W. Lee, C. H. Park, D. H. Kim, and M. H. Lee, (2001) Year. The Characteristics Of Deriving Control Of Crane [Deriving Read Driving]. *In:* Industrial Electronics, 2001. Proceedings. Isie 2001. Ieee International Symposium On,. Vol. **(2)**:734-739.

Ward, C., E. Stewart, H. Li, R. Goodall, C. Roberts, T.X. Mei, G. Charles and R. Dixon (2011) Condition Monitoring Opportunities Using Vehicle Based Sensors *Imeche Proceedings, Part F: Rail And Rapid Transit,* Vol. **(225):** No.2. 202-218.

Xia, F., C. Cole, and P. Wolfs, (2007) An Inverse Railway Wagon Model And Its Applications. *Vehicle System Dynamics,* 45**,** 583-605.

Yu, J. H. (2007) *Re-Adhesion Control For Ac Traction System In Railway Application.* Phd Thesis, The University of Leeds.